

# SYSTEM IDENTIFICATION AND CONTROL FOR THE SIRIUS HIGH-DYNAMIC DCM

R. M. Caliar<sup>†</sup>, R. R. Geraldes, M. A. L. Moraes, G. B. Z. L. Moreno, LNLS, Campinas, Brazil  
R. Faassen, T. A. M. Ruijl, R. M. Schneider, MI-Partners, Eindhoven, Netherlands

## Abstract

The monochromator is known to be one of the most critical optical elements of a synchrotron beamline. It directly affects the beam quality with respect to energy and position, demanding high stability performance and fine positioning control. The new high-dynamic double-crystal monochromator (HD-DCM) [1], prototyped at the Brazilian Synchrotron Light Laboratory (LNLS), was designed for the future X-ray undulator and superbend beamlines of Sirius [2], the new Brazilian 4th generation synchrotron. The next generation machines demand higher stability performance than at the previous ones, both at the accelerator and at the beamlines, requiring improved solutions to deal with factors such as high-power loads, power load variations, and vibration sources. This paper describes the system identification work carried out for enabling the motion control of the mechatronic parts composing the HD-DCM. The tests were performed in MATLAB/Simulink Real-Time (RT) environment, using a Speedgoat RT Performance Machine as a RT target. Sub-nanometric resolution and nanometric stability at 250 Hz closed loop bandwidth in a MIMO system were the main design targets. Frequency domain identification tools, control techniques and the first partial results are presented in this paper.

## INTRODUCTION

Sirius is a 4th generation synchrotron light source that is planned to be commissioned in mid-2018 in Brazil. Its low emittance (0.25 nm.rad) [3] makes it one of the world's brightest light sources of its kind. Due to the high quality of the photon beam, the Sirius beamlines are expected to present cutting-edge technologies in their fields.

In existing 3rd generation light sources X-ray beamlines, double-crystal monochromators (DCMs) are known to be one of the main current bottlenecks in their overall performance [4]. Indeed, the stability of this instrument affects both the energy selection and the position of the beam at the sample. Given the very small source sizes and large optical lever-arms in long beamlines, the DCMs must have the angular stability in the parallelism between crystals not greater than a few nanoradians to keep the source quality.

A new DCM concept started to be studied in 2015 at LNLS, after the output of the ESRF DCM Workshop in 2014. The target was to bring the parallelism stability levels to a new standard. To achieve this goal, it was decided to go to a totally innovative design, based on high-end mechatronics technology.

The mechanical design is briefly presented in the next section. Next, the hardware, the software, and the background theory are described. Finally, the first results of system identification and closed loop control are shown.

The partial results of the core of the HD-DCM (Fig. 1) were 9.2 nrad in relative pitch and roll, and 0.9 nm in relative gap (RMS values integrated from 0 to 2500 Hz). These results were obtained with the fixed Bragg angle and in air at room temperature.

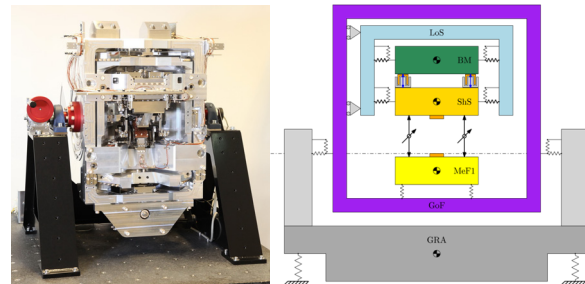


Figure 1: Left: core of the HD-DCM on dummy bearings; Right: HD-DCM core assembly schematic.

## HD-DCM DYNAMIC CONCEPT

The system consists of a vertically deflecting DCM with 18 mm beam offset. It has a main rotating frame (Gonio Frame, GoF in Fig. 1) that is guided by bearings at both sides and driven by an in-vacuum direct driver motor, with an angular working range from 3 to 60°. (These bearings are stiffly mounted to the HD-DCM vacuum chamber and supporting structure, represented by a granite frame (GRA) in Fig. 1.) The HD-DCM was designed with two crystal sets, originally planned to be Si(111) and Si(311) in the energy ranges from 2.3 to 38 keV and from 4.4 to 72 keV, respectively. The first crystals are stiffly mounted to a reference frame (Metrology Frame, MeF1 in Fig. 1), which is in turn stiffly fixed to the GoF. By having the main rotation axis coincident both with the incoming beam and the surface of the first crystals, the beam walk and thermal bump effects in the first crystals can be minimized. To handle the power load of about 100 W, with a power density of about 50 W/mm<sup>2</sup>, the crystals are indirectly cryocooled via compliant LN<sub>2</sub> feeding tubes.

Since the first crystals are fixed to the GoF, all the relative degrees of freedom (DoF) that are necessary for fine alignment between crystals are limited to the second crystals, which are also indirectly cryocooled simply by copper braids. Aiming at the highest repeatability and stability performance, only the essential DoF were implemented, namely: one translation for the gap between the crystals, which is necessary to keep constant beam offset; and two rotations, pitch and roll, for tuning. As a mechanism with nanometer level performance and several millimeter range

<sup>†</sup>ricardo.caliari@lnls.br

is hardly feasible within a single motion stage, a concept using a long-stroke stage and a short-stroke stage was implemented. The first is an auxiliary frame for the 10 mm gap stroke (Long Stroke Frame, LoS in Fig. 1), which is guided by an arrangement of leafsprings and driven by a servomotor, with micrometer accuracy. The latter is the high-dynamic module, consisting of: the reference frame to which the second crystals are stiffly mounted (Short Stroke Frame, ShS in Fig. 1), and a reaction mass (Balance Mass, BM in Fig. 1). Both are equally guided by an arrangement of leafsprings with respect to the LoS, providing the three necessary DoF for the second crystals in the ranges of  $\pm 2$  mm and  $\pm 2$  mrad. The control of the position of the second crystals with respect to the first crystals is based on an embedded interferometric system that directly measures the position between the MeF and the ShS. Finally, three contactless actuators (voice coils) between the ShS and the BM, control the position of the ShS.

Thus, in terms of dynamics, the main design targets were to have the ShS and BM weakly connected to the LoS via the leafsprings, i.e. decoupling at about 5 Hz, and to have internal frequencies in the MeF and in the ShS preferably above 1.5 kHz.

## SYSTEM ARCHITECTURE

The controller chosen to the first prototype was the xPC from Speedgoat, mainly because of its compatibility with the MATLAB/Simulink software, its high performance and flexibility. The system dynamic models were also developed using these software tools.

The xPC Controller was assembled for this project, but was intended to be as generic and flexible as possible and be used in future control prototypes to perform plant identifications and design controllers, as described in this work. The chosen IO boards have numerous ports (digital input and outputs, high-precision analog input and outputs and flexible temperature inputs), a programmable RT controller and a FPGA board. Details of this configuration are found in [5]. This prototyping control platform will be used until the first results of the HD-DCM are obtained in vacuum, with all subsystems integrated. After that, the designed controllers shall be implemented in the final control platform and its performance can be refined in the cRIO platform, from National Instruments, which was chosen as the standard controller for Sirius beamlines. This standardization decision is explained in [6].

A characteristic that is explored with these flexible controllers is the usage of linear amplifiers to drive the actuators. It means that, instead of using vendors' controllers (as in many motion control solutions, even with nanometric resolution [7]), which are normally limited to a PID controller and much smaller update rates (few kHz or even less), all controllers and system processes can be integrated in the same platform and use its high computational power to achieve, as in this project, at least 10 or 20 kHz update rate. They are also more flexible in the controller design and system identification, embedded signal processing and high precision and resolution signal generators (for example to generate trajectories).

## APPLIED TECHNIQUES

### System Identification

The system identification techniques [8] are based in time and frequency domain analyses and use mathematical and statistical tools to understand a real system and describe its dynamic behaviour. They are used in synchrotron facilities, including LNLS, for a long time mainly for the particles orbit control at the accelerator [9, 10].

The applied techniques are based on the linear behaviour of each system section in its operating conditions (frequency range and physical limitations). Thus, these Frequency Response Function (FRF) measurements are based on linear system assumptions. In practice, the FRF is the result from the division of the output signal Fast Fourier Transform (FFT) by the input signal FFT.

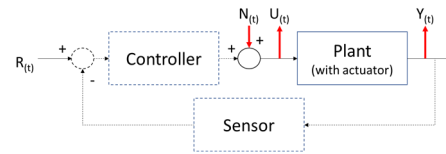


Figure 2: System identification techniques, injecting noise in open-loop and closed-loop (dashed lines) configurations. Inputs and outputs are described in the text.

This formulation is straightforward for an open-loop configuration, but Fig. 2 shows that it is also possible to identify the plant in closed-loop. This is especially convenient to use the control to keep the system within the so called “physical limits”, controlled by the reference  $R(t)$ . Its drawback is that a minimally suitable controller must be designed, meaning that a rough estimation of the system parameters is mandatory.

As seen in Fig. 2, the measured signals are: the plant input  $U(t)$  and output  $Y(t)$  signals. The input signal  $N(t)$  is injected just after the controller. Computing the transfer function from input to each output and manipulating this data makes it possible to measure the plant transfer function. The theory and proofs are found in the reference [8].

### Excitation Signals

Figure 2 shows that the presented techniques are based on injecting a well-known signal and monitoring a specific system output. It is important to highlight that both the amplitude and frequency ranges of the input signal must be limited to ensure that the system output is also within the desired ranges, i.e. above noise levels and below saturation. The correlations for amplitude and frequency range between the input and output signals are consequences of the linear system characteristics, as mentioned before.

These input signals can be divided in two groups, namely, non-deterministic (white noise and chirp sine) and deterministic signals (step sine and multisine). The time and frequency domain plots are shown in Fig. 3. The implications of each signal type are discussed below:

**Random noise** This signal can be found in Simulink as the “Band-Limited White Noise” block, and is also im-

plemented in many other software tools. It is based in computational methods to generate random numbers, with the spectral density distribution, i.e. amplitude and frequency characteristics, controlled via block parameters or complementary filters. Its random characteristic makes it unsuitable for the deterministic characterization approach that is proposed.

**Chirp sine** In this signal, a sinusoidal signal frequency varies linearly over time, normally with fixed amplitude and phase, as seen in Fig 3. The frequency linear variation is an advantage because one can derive the frequency from the time scale and this makes a wide frequency range to be performed in a relative small time. Due to these characteristics, this signal is largely used to identify electronic systems. In mechanical systems, however, transient conditions are more significant and higher damping and inertia lead to slower responses. Therefore, changing an input parameter (in this case the frequency) too fast and without averaging may be a problem to properly correlate the input and output signals. We classify this signal as non-deterministic due to its linear frequency variation characteristic, which means that the frequency is different for every time unit, implying that the system response at a given time may not be directly correlated with the instantaneous input frequency.

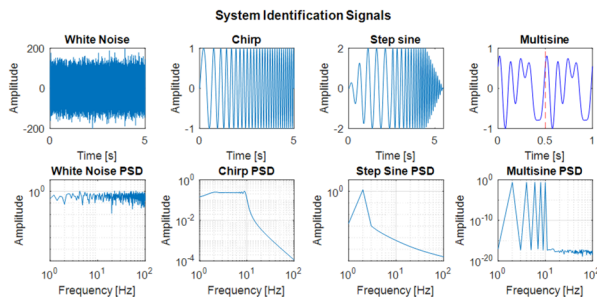


Figure 3: System identification signals: white noise, chirp, step sine and multisine. Its time and frequency domain representations.

**Step sine** In this method, the system is submitted to a harmonic input during some periods of the excitation signal. This well-known period precisely shows the system response from this specific frequency. After the specified time, the input frequency may change to the next discrete value. The time elapsed in each frequency minimizes the transient and accommodation effects, meaning that, with the help from statistics, the linear conditions of the system can be more well evaluated. The drawback, when comparing with the chirp signal, is the larger duration time. Another advantage of this technique is to have enough information to compute a frequency domain analysis for each frequency at the input. Some non-linearities, for example, are identified as a response in a frequency that is different from the excitation.

**Multisine** Figure 3 shows clearly the advantage of this method. With a single signal period, a deterministic frequency range can be characterized. This signal is a sum of a finite number of harmonic signals with the same amplitude in the frequency domain. The advantage of this

method is to have all frequency content in just one signal period. Statistics techniques can be applied here to enhance the method precision, minimize the transient influences and external random noise sources.

For the so-called deterministic signals, an amplitude ramp is normally used in the beginning and in end of the identification. This helps the system to gently start the movement and achieve the desired amplitude. This is depicted in Fig. 3, at the step sine time domain plot.

### Control

In control engineering, many researchers prefer a more statistical approach, others are based in machine learning, whereas some chose the study of machine operators to perform control in a fuzzy way [11]. The more traditional and deterministic approach is chosen for this work. The techniques presented here may not be optimal but ensure the stability and the convergence of the solutions with a mathematic formalism, as proven in [11].

These control tools are largely used in synchrotron facilities. In its majority, as in the general industry, simpler controllers and open-loop techniques are used, but the Fast Orbit Feedback Systems is a great example of the traditionally implementation of the referred classic and modern solutions [12,13]. The LNLS current machine, the so-called UVX, has also operated using the closed-loop control techniques for a long time [14].

The application of control techniques for light flexible structures started in the space industry, in the 60's [15] and is now spread over many other fields, as discussed also in [16]. The HD-DCM is the first step in bringing this knowledge to Sirius high-end beamline instrumentation. A brief description of each applied control technique and some of their characteristics are given, more precise formulations are seen in [11]:

**PID controller** By far the most used control solution in the industry, this controller is a composition of proportional, integral and derivative terms of a transfer function (traditionally called:  $K_p$ ,  $K_i$ ,  $K_d$ ). They can be tuned for each different application, aiming to apply an accurate and responsive correction to a control function.

**Lead-lag compensator** One of the most traditional compensation techniques, this gives the engineer the freedom to place a pole and a zero at any place, inside the imaginary plane (for example using the root locus graphic tool). The phase advance of the zero combined with the phase lag of the pole can be combined to increase the phase margin near the controller bandwidth.

**Integrator filter** This filter is applied normally at the lower frequencies to increase the open loop gain below the bandwidth.

**Low Pass filter** Largely used to avoid high-frequency noise, this filter drops the gain of the controller above a given frequency.

**Notch filter** This filter has the characteristic of dropping the controller gain at a certain frequency, but with

Content from this work may be used under the terms of the CC BY 3.0 licence (© 2017). Any distribution of this work must maintain attribution to the author(s), title of the work, publisher, and DOI.

minimum influence in the remaining spectrum. Two important aspects must be highlighted: firstly, the deeper the gain drop, the larger the phase influence in nearby frequencies, typically leading to phase margin loss; and secondly, care must be taken when notching a specific phenomenon, such as a vibration noise peak, because, if its frequency changes over time, the notch may not suppress it anymore, leading to stability loss. One can make the notch wider, to be robust for small frequency changes, but this leads to an even higher impact on phase loss than increasing the depth.

## RESULTS

Every element in the control loop of a system has an impact in its performance. Therefore, the control system of the HD-DCM has been developed in a systematic way, following a sequence of validation steps through which knowledge and confidence on the performance of the system have been gradually built up. By having a solid comprehension of the system characteristics, the control designer can take maximum advantage of the system capacity and may work more effectively on improvements. This process started with the investigation of the controller (latencies, digital/analog conversion impacts, etc), the amplifiers, the actuators and the sensors, continued with the identification of the mechanics, and finished with the design of the controller and the validation of its performance design targets.

These results are focused in the high-dynamic module, capable of controlling the fine parallelism of the two crystals in 3 DoF, as described before. The Long Stroke performance and its influence in the overall performance was also investigated, but the results will be published with the final results of the system.

### Electronics Characterization

For an ultimate performance, it is required that electronic limitations, such as non-linearities, latencies and noise levels of the controller, the amplifiers, the actuators and the sensors are known, and either compensated or kept below sufficiently low levels.

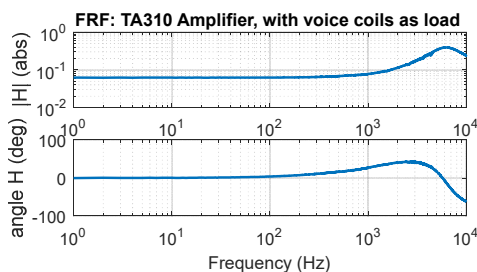


Figure 4: Frequency Response Function of the Trust Automation TA310 linear amplifier, with voice-coils as load.

The transfer function of every amplifier and acquisition board was measured using the previously described techniques for system identification with the most convenient selection of input and output signals. As an example, Fig. 4 shows the FRF of the Trust Automation TA310 linear amplifier that is used with the voice-coil actuators. This is the result of a multisine characterization having the controller

output voltage as the input signal and the amplifier output current as the output signal, which were measured with a voltmeter and a current meter, respectively. The curve proves its linearity within the BW and the absence of high frequency induced noise. The high frequency peak is due to an unbalanced load, which can be compensated at the controller.

Next, the noise floor of the acquisition boards and sensors were also investigated. As an example, Fig. 5 shows the noise floor of the Smaract Picoscale interferometric system for an in-air cavity at room temperature. The Power Spectrum Density (PSD), shows the noise distribution over the frequency range. For now, the 0.7 nm RMS is the most important limiting factor for the 0.9 nm shown in the partial results of stability performance of the HD-DCM in closed loop (see Fig.9). It is expected that this noise level will be reduced for the final application in vacuum.

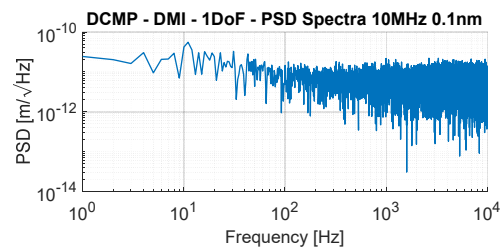


Figure 5: Interferometer noise floor PSD.

### Plant Identification

Using a MIMO approach, i.e., having the three voice-coils and three interferometers transformed to independent inputs and outputs representing the one translation and the two rotations of the ShS, different identification techniques were applied to the system to investigate its behaviour.

Firstly, multisine characterizations easily showed the expected FRF shape in all three DoF, with the low-frequency decoupling peak and high frequency peaks starting at 1200 Hz, suggesting that the mechanical design target had been achieved. Having the first plant identification, a simple controller could be implemented and then, step sine characterizations could be used to more accurately identify the flat portion (slope 0) of the lowest frequency range, i.e., the ShS characteristic stiffness lines for frequencies below the main decoupling peak. Next, step sine was also used above the decoupling peak frequency in the -40 dB/dec (slope -2) frequency range, which provides the ShS mass and moments of inertia. This region, between 20 and 1000 Hz, is critical to the system closed-loop behaviour near the controller bandwidth at 250 Hz.

Figure 6 shows the FRF from the real data. The non-diagonal terms lower magnitudes show that the system is well decoupled. In MATLAB, this is a system from Frequency Response Data (FRD), which means that each point in the plot is a measurement compiled as described in the System Identification section. The identified plant can be combined with the designed controller and its characteristics, such as stability and robustness, can be calculated, as described in the next section.

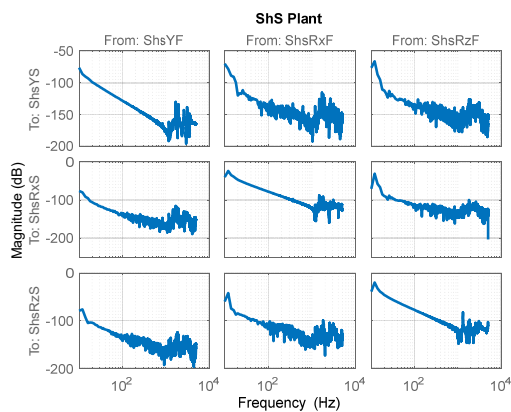


Figure 6: MIMO plant identification using single sine method.

### Controller Design

The controller was designed to be stable and robust (presently the phase margin is 28.8 degrees and the gain margin is 2.03), to reject noise at low frequencies (high open-loop gain below the bandwidth) and to suppress high frequency noise (low sensitivity peak). These characteristics were implemented using a lead-lag compensator and filters: an integrator at low frequencies, a low pass at high frequencies, and notches to suppress some well-known mechanical peaks, the ones near the low-pass cut-off frequency. These characteristics are shown in Fig. 7 and Fig. 8, where the controller, the sensitivity and the open-loop plots for the ShS in the three DoF are depicted.

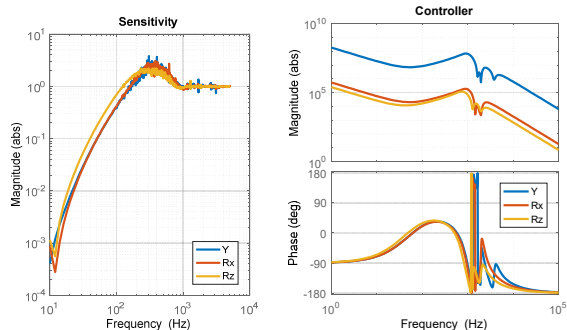


Figure 7: Sensitivity and controller for the ShS in the 3 DoF.

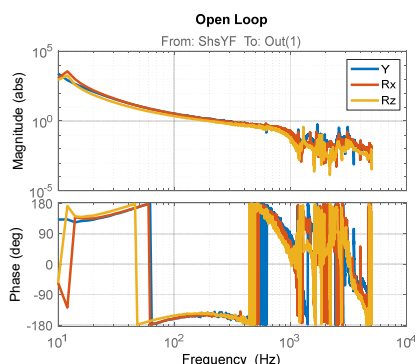


Figure 8: Open-loop plots of magnitude and phase for the ShS in the 3 DoF, showing the system dynamic performance under control.

### Partial Results

The in-position performance of the ShS is depicted in Fig. 9, in which the cumulated RMS position stability is shown as a function of frequency for all three DoF. This evaluation is made up to the Nyquist frequency, i.e. 10 kHz, for a 20 kHz closed-loop control frequency.

Regarding mechanical disturbances, the performance of the ShS will mainly suffer from the LN<sub>2</sub> flow induced vibrations [16], floor vibrations and excitations from the rotary stage and the LoS actuator [17]. The impact of such noise sources has been estimated using the analytical model and considered in the error budget during the development of the instrument, but still needs experimental confirmation. Naturally, these components may eventually affect the present design of the controller.

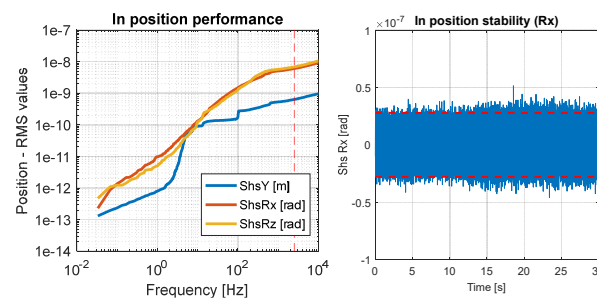


Figure 9: Left: Cumulated RMS position stability for all 3 directions under control. Right: Time domain plot, of Rx (relative pitch) direction, with 3 sigma value indicated.

### CONCLUSION

The new high-dynamic monochromator innovative concept was proved within the core of the instrument, showing its high stability performance: 9.2 nrad relative pitch and 0.9 nm relative gap (RMS values integrated from 0 to 2500Hz). These figures were achieved still with fixed Bragg angles, having the system in air and at room temperature, but numbers for the complete cryocooled system, including scanning performance, are expected by the end of 2017. Predictive modelling was shown to be mandatory for such a high-performance system, where no detail can be neglected, even in preliminary phases.

The system identification methods applied to the electronics hardware and the mechanical plant proved to be a very robust and an essential approach to be used in designing a proper controller for a high-end system. With them, the closed-loop control of the HD-DCM was successfully implemented following the most important design targets from the literature. Moreover, with these tools the implementation of a new controller using any new control design technique is also straightforward.

### ACKNOWLEDGEMENT

The authors would like to gratefully acknowledge the funding by the Brazilian Ministry of Science, Technology, Innovation and Communication and the contribution of the LNS team, the MI-Partners team and those of the synchrotron community who directly or indirectly build the path to this development.

## REFERENCES

- [1] R. R. Geraldés, R. M. Caliari, M. Saveri Silva, “Instrumento para movimentação e posicionamento de elementos ópticos com resolução e estabilidade mecânica nanométricas em linhas de luz”, PCT/BR2017/050262, 2017, Patent Application.
- [2] A. R. D. Rodrigues *et al.*, “Sirius Status Report”, in *Proc. IPAC'16*, Busan, Korea, May 2016, paper WEPOW001, pp. 2811-2814.
- [3] L. Liu, F. H. de Sá, and X. R. Resende, “A new optics for Sirius,” in *Proc. IPAC'2016*, pp. 3413–3415.
- [4] R.R. Geraldés, R.M. Caliari, G.B.Z.L. Moreno, M.J.C. Ronde, T.A.M. Ruijl, and R.M. Schneider, “Mechatronics Concepts for the New High-Dynamics DCM for Sirius”, in *Proc. 9th Edition of the Mechanical Engineering Design of Synchrotron Radiation Equipment and Instrumentation Conf. (MEDSI'16)*, Barcelona, Spain, Sep. 2016, paper MOPE19, pp. 44-47, ISBN: 978-3-95450-188-5.
- [5] G. Moreno *et al.*, “Rapid control prototyping tool for the Sirius high dynamic DCM”, presented at ICALEPCS 2017, Barcelona, Spain, Sep. 2017, this conference.
- [6] M. Moraes *et al.*, “A control architecture proposal for Sirius beamlines”, presented at ICALEPCS 2017, Barcelona, Spain, Sep. 2017, this conference.
- [7] L. Ducotte, J.M. Clement, H. Gleyzolle, and J. Wright, “The New ID11 Nanoscope End-Station - A Nano-Tomography Scanner”, presented at the *9th Edition of the Mechanical Engineering Design of Synchrotron Radiation Equipment and Instrumentation Conf. (MEDSI'16)*, Barcelona, Spain, Sep. 2016, paper TUBA02, unpublished.
- [8] R. Pintelon, J. Schoukens, *System Identification: A Frequency Domain Approach*. Hoboken, NJ, USA: Wiley, 2012
- [9] J. Pfungstener *et al.*, “Performance comparison of different system identification algorithms for FACET and ATF2”, in *Proc. IPAC2013*, Shanghai, China, Sep. 2013, paper TUPME050.
- [10] D. O. Tavares, D. R. Grossi, “System identification and robust control for the LNLS UVX Fast Orbit Feedback”, in *Proc. ICALEPCS2015*, Melbourne, Australia, Aug. 2015, paper MOC3O04.
- [11] K. Ogata, *Modern Control Engineering*. Upper Saddle River, NJ, USA: Prentice Hall, 1997.
- [12] J. Rowland *et al.*, “Status of the Diamond Fast Orbit Feedback System”, in *Proc. ICALEPCS'07*, paper RPPA10.
- [13] S. Gayadeen *et al.*, “Fast Orbit Feedback Control in Mode Space”, in *Proc. ICALEPCS'13*, paper THMIB07.
- [14] L. Sanfelici *et al.*, “LNLS Fast Orbit Feedback System”, in *Proc. PAC'11*, paper MOP263.
- [15] A. Preumont, *Vibration Control of Active Structures, An Introduction*. Berlin, GER: Springer, 2011.
- [16] R.M. Caliari *et al.*, “Studies on Flow-Induced Vibrations for the New High-Dynamics DCM for Sirius”, in *Proc. 9th Edition of the Mechanical Engineering Design of Synchrotron Radiation Equipment and Instrumentation Conf. (MEDSI'16)*, Barcelona, Spain, Sep. 2016, paper MOPE02, pp. 8-11, ISBN: 978-3-95450-188-5.
- [17] P. Kristiansen, J. Horbach, R. Doehrmann, J. Heuer *et al.*, “Vibration Measurements of high-heat-load monochromators for DESY PETRA III extension”. *J. Synchrotron Rad.*, vol. 22, pp. 879-885, Jul. 2015